

Topologically protected subdiffusive transport in two-dimensional fermionic wires

Junaid Majeed Bhat^{1,2}

¹*Department of Physics, Faculty of Mathematics and Physics,
University of Ljubljana, 1000 Ljubljana, Slovenia*

²*International Centre for Theoretical Sciences,
Tata Institute of Fundamental Research, Bengaluru, 560089, India*

(Dated: October 13, 2023)

The conductance at the band edges of one-dimensional fermionic wires, with N sites, has been shown to have subdiffusive ($1/N^2$) behavior. We investigate this issue in two-dimensional fermionic wires described by a hopping model on an $N_x \times N_y$ rectangular lattice comprised of vertical chains with a Hermitian intra-chain and inter-chain hopping matrices given by H_0 and H_1 , respectively. We study particle transport using the non-equilibrium Green's function formalism, and show that the asymptotic behavior of the conductance, $T(\omega)$, at the Fermi level ω , is controlled by the spectrum of a dimensionless matrix $A(\omega) = (-\omega + H_0)H_1^{-1}$. This gives three simple conditions on the spectrum of $A(\omega)$ for observing ballistic, subdiffusive, and exponentially decaying $T(\omega)$ with respect to N_x . We show that certain eigenvalues of $A(\omega)$ give rise to subdiffusive contributions in the conductance, and correspond to the band edges of the isolated wire. We demonstrate that the condition for observing the subdiffusive behavior can be satisfied if $A(\omega)$ has nontrivial topology. In that case, a transition from ballistic behavior to subdiffusive behavior of the conductance is observed as the hopping parameters are tuned within the topological regime. We argue that at the transition point, different behaviors of the conductance can arise as the trivial bulk bands of $A(\omega)$ also contribute subdiffusively. We illustrate our findings in a simple model by numerically computing the variation of the conductance with N_x . Our numerical results indicate a different subdiffusive behavior ($1/N_x^3$) of the conductance at the transition point. We find the numerical results in good agreement with the theoretical predictions.

I. INTRODUCTION

Electronic transport in mesoscopic systems has been extensively explored for several decades now¹⁻⁴. However, new and interesting results are discovered in very simple models even after decades of research. One example would be the exotic transport characteristics of topological insulators and superconductors⁵⁻¹⁰ which have taken a central stage in modern quantum condensed matter¹¹⁻¹⁵. They are of interest as they possess the ability to carry dissipationless current via robust edge modes. These modes are protected from symmetry-preserving weak disorders as they are gapped from the bulk bands of the system. In one dimension, the simplest examples of a topological insulator and a topological superconductor are the Su-Schrieffer-Heeger model (SSH)^{16,17}, which describes poly-acetylene, and the Kitaev chain¹⁸, respectively. In two dimensions the Haldane model¹⁹, Bernevig, Hughes and Zhang model (BHZ)²⁰, and Kane-Mele model¹⁴ are known to possess non trivial band topology. Some of these models have been realized in different experimental setups^{21,22}.

Another very recent example is the work of Refs. 23 and 24 on the scaling of the conductance with system size in 1D fermionic wires at the band edges of the wire. It was found that a universal subdiffusive behavior of the conductance is observed if the Fermi level of the reservoirs is set at the band edges of the isolated fermionic wire. Therefore, the subdiffusive behavior separates the transition from ballistic to exponential decay of the conductance as one tunes the Fermi level of the

reservoirs from inside to outside the energy band. The band-structure of nearest neighbor fermionic wire with translation symmetry can be obtained from 2×2 transfer matrices²⁵⁻²⁷ and the subdiffusive behavior arises from the non-diagonalizability of this matrix. Similar peculiarities in the behavior of the wave functions near the band edges have been reported in earlier works also²⁸⁻³⁰.

In this paper, we show that the interplay of the above two examples reveals very interesting physics in two dimensions. We first look at the problem of the scaling of the conductance at the band edges in two dimensions, which to our knowledge has not been explored so far. To do that, we consider a fermionic wire described by a hopping model on a rectangular lattice ($N_x \times N_y$). We think of the wire to be comprised of N_x vertical chains of length N_y , and for simplicity we assume a Hermitian intra-chain as well as inter-chain hopping matrices H_0 and H_1 , respectively. We use the non-equilibrium Green's function formalism (NEGF)^{1,4,8,10} formalism to explore the asymptotic behavior of conductance at the Fermi level ω with respect to N_x , and find this behavior is controlled by the spectrum of a matrix, $A(\omega) = (-\omega + H_0)H_1^{-1}$. The Hermiticity of H_0 and H_1 , implies $A(\omega)$ is pseudo Hermitian with respect to H_1 . Such matrices have been found important in different problems of physics³¹⁻³⁸. Our work uncovers an interesting connection of such matrices with the transport in two-dimensional fermionic wires.

We find that the real eigenvalues of $A(\omega)$ of magnitude 2 lead to subdiffusive ($1/N_x^2$) contributions in the conductance, and correspond to the band edges of the isolated wire. Other real eigenvalues of magnitudes less

than and greater than 2 give rise to ballistic and exponentially decaying conductance with respect to N_x , and correspond to energies within and outside the bands of the isolated wire, respectively. The condition for observing subdiffusive behavior then reads that $A(\omega)$ has at least one eigenvalue of magnitude 2, and simultaneously all the other real eigenvalues greater than 2. This condition implies that the subdiffusive behavior would be seen only at the band edges of the isolated wire that do not lie within any other bands of the system. Therefore, as the positions of other bands of the isolated wire are tuned with respect to the edge of a particular band a ballistic to subdiffusive transition in the behavior of the conductance occurs. Since the Fermi level is kept fixed at some band edge, this band edge should remain fixed as the positions of the other bands are tuned by varying the parameters of H_0 and H_1 . We present a toy example in $2 \times N_x$ ladders where this transition occurs.

Interestingly, we find that if $A(\omega)$ is topologically non-trivial and the eigenvalues of topological modes of $A(\omega)$ are fixed at the value 2, then the transition from ballistic to subdiffusive ($1/N_x^2$) behavior occurs within the topologically nontrivial parameter regimes. In this case, the subdiffusive behavior is due to the topological modes, and therefore it possesses the same topological protection as the modes themselves. In contrast, for the parameter regimes where $A(\omega)$ is topologically trivial, a usual transition from ballistic to exponential decay of the conductance exists. We refer to the two transitions as the subdiffusive and exponential transitions, respectively. At the transition points, novel behaviors of the conductance can arise for thermodynamically large N_y . This is because at these points the bulk bands of $A(\omega)$ also contribute subdiffusively.

We illustrate our theoretical expectations by considering a simple model where $H_1 = \eta I$ and H_0 is the Hamiltonian of the SSH chain with a constant chemical potential. We numerically compute the behaviors of the conductance for large N_x and N_y for this model using an iteration method based on the Dyson equation for the Green's functions^{39,40}. Our numerical computations of the conductance agree with the theoretical expectations away from the transition points. At the transition points, our numerical computations indicate a different subdiffusive behavior ($1/N_x^3$) in the limit of $N_y \rightarrow \infty$.

This paper is structured as follows: Sec. II introduces the details of the wire Hamiltonian, the Hamiltonian of the reservoirs, and their couplings with the wire. In the next section, Sec. III, we discuss a simplification of the NEGF conductance formula from which its asymptotics with N_x become explicit in terms of the spectrum of $A(\omega)$. In the next section Sec. IV, we discuss the conditions for observing the different behaviors of the conductance namely ballistic, subdiffusive, and exponential decay. In section Sec. V, we discuss how the subdiffusive transition can occur in the parameters of the topological regime, if $A(\omega)$ has a nontrivial topology. In the penultimate section, we look at a simple model and discuss

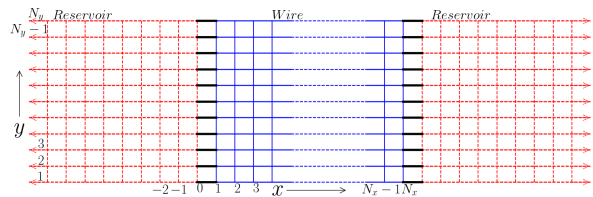


FIG. 1. Schematic of the wire in contact with the reservoirs along the left and right edges. This figure corresponds to the case where the hopping matrices, H_0 , H_1 , and \tilde{H}_0 allow only nearest neighbor hopping between the sites of the entire system.

the subdiffusive and the exponential transitions in this case. We also discuss the effects of disorder on the subdiffusive behavior. We then present numerical results for the conductance of this model at $\omega = 0$ to confirm our expectations from the theory. Our numerical computations agree well with the theoretical expectations away from the transition points. We also present numerical results on the conductance at the transition points, where we find a $1/N_x^3$ subdiffusive behavior for thermodynamically large N_y . We conclude in Sec VII.

II. MODEL

We consider the wire Hamiltonian to be given by a tight-binding model defined on a rectangular lattice of size $N_x \times N_y$. Let us call the creation and annihilation operators at the site (x, y) as $\psi^\dagger(x, y)$ and $\psi(x, y)$, respectively. We consider the wire in contact with two external reservoirs at the two opposite edges at $x = 1$ and $x = N_x$. The two reservoirs are taken to be metallic leads that are semi-infinite in the x -direction and of width N_y in the y -direction. These are modeled as 2D tight-binding Hamiltonians which we refer to as \mathcal{H}_L and \mathcal{H}_R . We label the corresponding annihilation and creation operators as $\phi_{L/R}(x, y)$ and $\phi_{L/R}^\dagger(x, y)$, where L and R label the left and the right lead, respectively. Free boundary conditions are imposed at the horizontal edges of the reservoir and the system at $y = 1$ and $y = N_y$ respectively. The contacts between the wire and the reservoirs are themselves modeled as tight-binding Hamiltonians, \mathcal{H}_{WL} and \mathcal{H}_{WR} . The full Hamiltonian of the wire and the reservoirs is therefore given by:

$$\mathcal{H} = \mathcal{H}_L + \mathcal{H}_{LW} + \mathcal{H}_W + \mathcal{H}_{RW} + \mathcal{H}_R, \quad (1)$$

where the individual Hamiltonians of the wire, the contents, and the reservoirs are given by,

$$\begin{aligned}\mathcal{H}_W &= \sum_{x=1}^{N_x} \Psi^\dagger(x) H_0 \Psi(x) \\ &+ \sum_{x=1}^{N_x-1} \Psi^\dagger(x) H_1 \Psi(x+1) + \Psi^\dagger(x+1) H_1 \Psi(x),\end{aligned}\quad (2)$$

$$\mathcal{H}_{LW} = \eta_c (\Psi^\dagger(1) \Phi_L(0) + \Phi_L^\dagger(0) \Psi(1)), \quad (3)$$

$$\mathcal{H}_{RW} = \eta_c (\Psi^\dagger(N_x) \Phi_R(N_x+1) + \Phi_R^\dagger(N_x+1) \Psi(N_x)), \quad (4)$$

$$\begin{aligned}\mathcal{H}_L &= \sum_{x=-\infty}^0 \Phi_L^\dagger(x) \tilde{H}_0 \Phi_L(x) \\ &+ \eta_{bx} \sum_{x=-\infty}^{-1} \Phi_L^\dagger(x) \Phi_L(x+1) + \Phi_L^\dagger(x+1) \Phi_L(x),\end{aligned}\quad (5)$$

$$\begin{aligned}\mathcal{H}_R &= \sum_{x=N_x+1}^{\infty} \Phi_R^\dagger(x) \tilde{H}_0 \Phi_R(x) \\ &+ \eta_{bx} \sum_{x=N_x+1}^{\infty} \Phi_R^\dagger(x) \Phi_R(x+1) + \Phi_R^\dagger(x+1) \Phi_R(x).\end{aligned}\quad (6)$$

We have defined column vectors $\Psi(x)$, and $\Phi_{L/R}(x)$ of N_y components with the y^{th} component given by the operators $\psi(x, y)$ and $\phi_{L/R}(x, y)$, respectively. These define the annihilation operators of a single chain of length N_y located at the position x . H_0, \tilde{H}_0 are the intra-chain hopping matrices inside the wire and the reservoirs, respectively. The inter-chain hopping matrix for the wire is taken to be H_1 , while the same is assumed to be $\eta_{bx} I$ for the reservoirs. Note that we have taken the reservoir Hamiltonians to be the same, and H_1 is assumed to be Hermitian and invertible. The couplings at the contacts are assumed to be of strength η_c . A schematic of the geometry with H_0, H_1 , and \tilde{H}_0 which only allow hoppings between nearest neighbor sites of the lattice is shown in Fig. 1.

Before moving to the next section to discuss the conductance of the wire within the NEGF formalism, it is instructive to note that the bands of the isolated wire for $N_x \rightarrow \infty$ and finite N_y are given by diagonalizing the matrix $H_0 + 2H_1 \cos(k_x)$ where k_x is the wave vector in the x direction. Therefore, the wire can have a maximum have N_y number of bands.

III. CONDUCTANCE IN THE THERMODYNAMIC LIMIT

The conductance for the system is given in terms of the nonequilibrium Green's function defined as^{4,10},

$$G^+(\omega) = \frac{1}{\omega - H_W - \Sigma_L(\omega) - \Sigma_R(\omega)}, \quad (7)$$

where $\Sigma_L(\omega)$ and $\Sigma_R(\omega)$ are the self energy corrections due to the reservoirs, and H_W is the full hopping matrix of the wire given by,

$$H_W = \begin{pmatrix} H_0 & H_1 & 0 & 0 & \dots & 0 & 0 \\ H_1 & H_0 & H_1 & 0 & \dots & 0 & 0 \\ 0 & H_1 & H_0 & H_1 & \dots & 0 & 0 \\ \vdots & \vdots & \vdots & \ddots & & \vdots & \vdots \\ \vdots & \vdots & \vdots & & \ddots & \vdots & \vdots \\ \vdots & \vdots & \vdots & \dots & H_1 & H_0 & H_1 \\ 0 & 0 & 0 & \dots & \dots & H_1 & H_0 \end{pmatrix}. \quad (8)$$

With the reservoirs kept at zero temperature and their chemical potentials chosen to have a small bias around the value ω , the conductance of the wire at the Fermi level ω is then given in terms of $G^+(\omega)$ as,

$$T(\omega) = 4\pi^2 \text{Tr}[G^+(\omega) \Gamma_R(\omega) G^-(\omega) \Gamma_L(\omega)], \quad (9)$$

where $G^-(\omega) = [G^+(\omega)]^\dagger$ and $\Gamma_{L/R} = (\Sigma_{L/R}^\dagger - \Sigma_{L/R})/(2\pi i)$. Since the contacts with the reservoirs are only along the edges i.e. at $x = 1$, and $x = N_x$, the above trace can be computed as,

$$T(\omega) = 4\pi^2 \text{Tr}[G_{1N_x}^+ \Gamma G_{N_x1}^- \Gamma], \quad (10)$$

where $G_{1N_x}^+[y, y'] = G^+(\omega)[x = 1, y; x' = N_x, y']$, $G_{N_x1}^- = [G_{1N_x}^+]^\dagger$ are block matrices which form the full Green's function $G^+(\omega)$. Similarly, $\Gamma[y, y'] = \Gamma_R[N_x, y; N_x, y'] = \Gamma_L[1, y; 1, y']$ are the non-zero block matrices of Γ_L and Γ_R , respectively. We need to find the $(1, N_x)$ block, $G_{1N_x}^+$ of the Green's function, $G^+(\omega)$, we do this by the transfer matrix approach. From the identity $G^+(\omega)(\omega - H_W - \Sigma_L - \Sigma_R) = I$, one can exploit the block tridiagonal structure of H_W to obtain the following equations for the inverse of the block components, G_{1i}^+ , of the Green's function $G^+(\omega)$,

$$G_{11}^+(\omega - H_0 - \Sigma) + G_{12}^+ H_1 = I, \quad (11)$$

$$G_{1,i-1}^+ H_1 + G_{1,i}^+(\omega - H_0) + G_{1,i+1}^+ H_1 = 0; \quad 1 < i < N_x, \quad (12)$$

$$G_{1,N_x-1}^+(\omega - H_0 - \Sigma) + G_{1N_x}^+ H_1 = 0. \quad (13)$$

Using the transfer matrix approach we can show

$$(I \quad G_{11}^+) = (G_{1N_x}^+ \quad 0) \Omega_R \Omega^{N_x} \Omega_L, \quad (14)$$

where,

$$\Omega_R = \begin{pmatrix} I & \Sigma H_1^{-1} \\ 0 & 0 \end{pmatrix}, \Omega_L = \begin{pmatrix} -H_1 & 0 \\ -\Sigma & I \end{pmatrix},$$

$$\text{and, } \Omega = \begin{pmatrix} (-\omega + H_0)H_1^{-1} & I \\ -I & 0 \end{pmatrix}. \quad (15)$$

Σ is an $N_y \times N_y$ matrix with components given by $\Sigma[y, y'] = \Sigma_R[N_x, y; N_x, y'] = \Sigma_L[1, y; 1, y']$. It can be shown that $\Sigma = U_L \Sigma_D U_L^\dagger$, where Σ_D is a diagonal matrix with components given by,

$$\Sigma_D[k, k] = \begin{cases} \frac{\eta_c^2}{\eta_{bx}} \left[\frac{\omega - \chi_k}{2\eta_{bx}} + i \sqrt{1 - \left(\frac{\omega - \chi_k}{2\eta_{bx}} \right)^2} \right]; & |\omega - \chi_k| < 2\eta_{bx}, \\ \frac{\eta_c^2}{\eta_{bx}} \left[\frac{\omega - \chi_k}{2\eta_{bx}} - \sqrt{\left(\frac{\omega - \chi_k}{2\eta_{bx}} \right)^2 - 1} \right]; & \omega - \chi_k > 2\eta_{bx}, \\ \frac{\eta_c^2}{\eta_{bx}} \left[\frac{\omega - \chi_k}{2\eta_{bx}} + \sqrt{\left(\frac{\omega - \chi_k}{2\eta_{bx}} \right)^2 - 1} \right]; & \omega - \chi_k < -2\eta_{bx}. \end{cases} \quad (16)$$

U_L is the unitary transformation that diagonalizes the intra-chain hopping matrix \tilde{H}_0 of the reservoirs and its eigenvalues are given by χ_k , $k = 1, 2, \dots, N_y$.

Let U be such that $A(\omega) = (-\omega + H_0)H_1^{-1} = U\Lambda(\omega)U^\dagger$, where $\Lambda(\omega)$ is a diagonal matrix comprising of the eigenvalues of $A(\omega)$. Using this we have,

$$\Omega^{N_x} = \begin{pmatrix} U & 0 \\ 0 & U \end{pmatrix} \begin{pmatrix} \Lambda(\omega) & I \\ -I & 0 \end{pmatrix}^{N_x} \begin{pmatrix} U^\dagger & 0 \\ 0 & U^\dagger \end{pmatrix} \quad (17)$$

$$= \begin{pmatrix} U & 0 \\ 0 & U \end{pmatrix} \begin{pmatrix} P_{N_x} & P_{N_x-1} \\ -P_{N_x-1} & -P_{N_x-2} \end{pmatrix} \begin{pmatrix} U^\dagger & 0 \\ 0 & U^\dagger \end{pmatrix}, \quad (18)$$

where P_N is a diagonal matrix comprising of diagonal entries given by p_N^k , obtained via the iteration,

$$p_{n+1}^k = \lambda_k(\omega)p_n^k - p_{n-1}^k; \quad p_0^k = 1, \text{ and } p_1^k = \lambda_k(\omega). \quad (19)$$

With this simplification of Ω we get,

$$G_{1N_x}^+ = -UG'_{1N_x}U^\dagger, \quad (20)$$

$G'_{1N_x} = [P_{N_x}H'_1 + \Sigma'H_1'^{-1}P_{N_x-1}H'_1 + P_{N_x-1}\Sigma' + \Sigma'H_1'^{-1}P_{N_x-2}\Sigma']^{-1}$. We have expressed Σ and H_1 in the diagonal basis of $A(\omega)$ as $\Sigma' = U^\dagger\Sigma U$, and $H'_1 = U^\dagger H_1 U$. This equation can be substituted in Eq. (10) to obtain the conductance of the wire.

We now assume a weak coupling limit given by $\frac{\eta_c}{\eta_{bx}} \ll 1$, then the leading behavior of the $G'_{1N_x} \approx -H_1'^{-1}P_{N_x}^{-1}$ because the self energy terms are proportional to η_c^2/η_{bx} . Since $P_{N_x}^{-1}$ is diagonal the conductance simplifies to the following simple expression,

$$T(\omega) \approx 4\pi^2 \sum_{k,k'} \frac{\mathcal{L}_{k,k'}}{p_{N_x}^k p_{N_x}^{*k'}}, \quad (21)$$

where $\mathcal{L}_{k,k'} = \Gamma'_{k,k'}(H_1'^{-1}\Gamma'H_1'^{-1})_{k',k}$. For large N_y the sum over k, k' can be replaced by an integral with an

appropriate density, $g(\lambda, \omega)$ of real eigenvalues of $A(\omega)$. We show in appendix A that the complex eigenvalues always contribute an exponentially small amount in the conductance for large N_x , and therefore we ignore them here. $g(\lambda, \omega)$ could in principle be obtained from the densities, $g_0(\mu)$ and $g_1(\mu)$, of the eigenvalues of H_0 and H_1 as $A(\omega)$ is completely specified by them. However, the transformation from the spectral density of H_0 , and H_1 , to the spectral density of $A(\omega)$ is very involved for arbitrary H_0 and H_1 . Nevertheless, in the continuum limit, we can write the conductance expression in terms of $g(\lambda, \omega)$ as,

$$T(\omega) = 4\pi^2 \int d\lambda d\lambda' g(\lambda, \omega) g(\lambda', \omega) \frac{|\mathcal{L}(\lambda, \lambda')|^2}{p_{N_x}(\lambda)p_{N_x}(\lambda')}, \quad (22)$$

where we replaced the dependences on the indices k and k' , with functions of λ and λ' , respectively. A natural question to address here is how the density $g(\lambda, \omega)$ is related to the density of states, $g_W(E)$, of the isolated wire in the thermodynamic limit as we would expect the latter to play a role in the conductance expression. We show that these two densities are related to each other for the case where H_0 and H_1 have translational symmetry and commute. In that case, the spectrum of the isolated wire is given by $\epsilon(k_x, k_y) = \mu_0(k_y) + 2\cos(k_x)\mu_1(k_y)$. k_x , k_y being the wave vectors in the x and y direction, respectively, and $\mu_0(k)$ and $\mu_1(k)$ are the spectrum of the matrices H_0 and H_1 , respectively. The density of states of the wire $g_W(E)$ can be obtained from the following integral,

$$g_W(E) = \int dk_x dk_y \tilde{g}_W(k_x, k_y) \quad (23)$$

$$= \int dk_x dk_y \delta(E - \mu_0(k_y) - 2\cos(k_x)\mu_1(k_y)).$$

On the other hand, we can write the eigenvalues of $A(\omega)$ as $\lambda_{k_y} = (-\omega + \mu_0(k_y))/\mu_1(k_y)$, from which the density

can be computed by doing the following integral,

$$g(\lambda, \omega) = \int dk_y \delta(\omega - \mu_0(k_y) + \mu_1(k_y)\lambda). \quad (24)$$

On comparing the two equations for the densities, we see that if $k_x = \arccos(-\lambda/2)$ and $\omega = E$, then

$$g(\lambda, \omega) = \sin(k_x(\lambda)) \int dk_y \tilde{g}_W(k_x(\lambda), k_y). \quad (25)$$

So, $g(\lambda, \omega)$ is the total density of the states of the isolated wire in the thermodynamic limit at a particular k_x . The two densities should also be related for arbitrary H_0 and H_1 but it seems nontrivial to relate the two.

IV. BEHAVIORS OF THE CONDUCTANCE AT LARGE N_x

The Hermiticity of H_0 and H_1 implies that $A^\dagger(\omega) = H_1^{-1}A(\omega)H_1$, and therefore $A(\omega)$ is pseudo Hermitian with respect to H_1 . It can have complex eigenvalues in general but for this section and the rest of the paper, we assume a real spectrum of $A(\omega)$ to discuss the behaviors of the conductance at large N_x . We relegate the case of complex eigenvalues, which isn't very different, to the appendix A.

From Eq. 21, we note that the behavior of the conductance with respect to N_x is controlled by the N_y number of iteration equations for p_n^k defined at each eigenvalue $\lambda_k(\omega)$ of the matrix $A(\omega)$. The solution for the iteration can be expressed in terms of the 2×2 transfer matrices given by,

$$\begin{pmatrix} p_{n+1}^k \\ p_n^k \end{pmatrix} = M^n \begin{pmatrix} p_1^k \\ p_0^k \end{pmatrix}, \quad (26)$$

where, $M = \begin{pmatrix} \lambda_k(\omega) & -1 \\ 1 & 0 \end{pmatrix}$. It is straightforward to see if $\lambda_k(\omega) \neq 2$, then $p_{N_x}^k = \sin(q^k(N_x + 1))/\sin(q^k)$, where, $q^k = \arccos[\frac{\lambda_k(\omega)}{2}]$. Note that for $|\lambda_k(\omega)| < 2$, p_n^k is oscillatory in n while for $|\lambda_k(\omega)| > 2$, p_n^k grows exponentially. If $\lambda_k(\omega) = 2$, then the matrix M becomes nondiagonalizable and $p_{N_x}^k = N_x + 1$. Depending on the behaviors of all the $p_{N_x}^k$'s with N_x , which are in turn determined by the spectrum of $A(\omega)$, we can have three possible behaviors of the conductance in the limit, $N_x \rightarrow \infty$. These are given by,

- Ballistic ($T(\omega) \sim e^{i\alpha N_x}$, α is real): The ballistic contribution comes from $\lambda_k(\omega)$'s with absolute values less than 2, since for such eigenvalues $p_{N_x}^k \sim e^{\pm i q^k N_x}$. Moreover, the conductance is proportion to the inverse of $p_{N_x}^k$, and therefore the ballistic contribution dominates the transport as other contributions are suppressed in the limit $N_x \rightarrow \infty$. Hence, a ballistic behaviour of the conductance occurs if at least one of the $\lambda_k(\omega)$'s has a magnitude

of less than 2. This condition is always satisfied by ω lying within a band of the bulk spectrum of the wire for arbitrary H_0 and H_1 . This is readily seen if $[H_0, H_1] = 0$, then $\lambda_k(\omega) = (-\omega + \mu_0^k)/\mu_1^k$, where μ_0^k and μ_1^k are the k^{th} eigenvalues of H_0 and H_1 , respectively. Hence, for a particular k , $|\lambda_k(\omega)| < 2$ gives $E_-^k < \omega < E_+^k$, where E_+^k and E_-^k are the maximum and minimum of $\mu_0^k \pm 2\mu_1^k$, respectively. Note that E_\pm^k are exactly the band edges of the k^{th} band of the bulk spectrum, given by $\mu_0^k + 2\cos(k_x)\mu_1^k$, of the isolated wire. We consider the case where H_0 and H_1 do not commute in the appendix B. If all the eigenvalues of $A(\omega)$ contribute ballistically, we see that the integration over λ and λ' in Eq. (22) can be restricted over the values of with $|\lambda| < 2$, and we have,

$$T_b(\omega) = \int_{-2}^2 \int_{-2}^2 d\lambda d\lambda' g(\lambda, \omega) g(\lambda', \omega) \frac{|\mathcal{L}(\lambda, \lambda')|^2}{p_{N_x}(\lambda) p_{N_x}(\lambda')}. \quad (27)$$

- Exponential decay ($T(\omega) \sim e^{-2\alpha N_x}$, $\alpha > 0$): This behaviour occurs when all the $\lambda_k(\omega)$'s have magnitude greater than 2. In that case, every $p_{N_x}^k$ will grow exponentially with N_x , and therefore contribute an exponentially small amount in the conductance. A similar analysis as in the ballistic case gives that the exponential decay occurs only at $\omega > E_+^k$ or $\omega < E_-^k$ for $[H_0, H_1] = 0$. Therefore, we see exponentially decaying behavior outside the energy bands of the isolated wire. For this case the leading behavior of the conductance is given by the eigenvalue, λ_{min} with minimum $\text{Im}[\arccos(\lambda_k/2)]$. Using this fact in Eq.(22), we have

$$T_e(\omega) \sim g^2(\lambda_{min}, \omega) e^{-2|\text{Im}\{\arccos \lambda_{min}\}|N_x}. \quad (28)$$

- Subdiffusive ($T(\omega) \sim 1/N_x^2$): The subdiffusive contribution comes from $\lambda_k(\omega)$'s of absolute value equal to 2 as for such eigenvalues $p_{N_x}^k \sim N_x$, and therefore their contribution in conductance is proportional to $1/N_x^2$. Hence, to see the subdiffusive behavior, one of the $\lambda_k(\omega)$'s should have a magnitude of 2 and at the same time, all the other eigenvalues should be of magnitude greater than 2. The latter part of the condition is to ensure that there are no eigenvalues which contribute ballistically. Otherwise the contribution from such eigenvalues will dominate the behavior of the conductance at large N_x . In one dimension, this condition is trivially satisfied for ω corresponding to the band edges of the 1D wire with translational symmetry and nearest neighbor hoppings. Once again if $[H_0, H_1] = 0$, then $\lambda_{k*}(\omega) = 2$ implies that ω is the same as the band edges, E_\pm^{k*} , of the isolated wire. In the appendix B, we show that this is true even when H_0 and H_1 do not commute. Note that the subdiffusive condition will only be satisfied at

the band edges, E_{\pm}^{k*} that do not lie within any other energy bands of the spectrum of the isolated wire. The subdiffusive contribution of the band edges lying within any other band would be subdued due to the ballistic contribution of the other band. For the subdiffusive case, only the modes at $\lambda = 2$ contribute in Eq. 22 and therefore,

$$T_s(\omega) \sim \frac{1}{p_{N_x}^2(2)} \sim \frac{1}{N_x^2}. \quad (29)$$

We refer to the eigenvalues of $A(\omega)$ that give rise to the three different behaviors as ballistic, exponential, and subdiffusive eigenvalues, respectively. The fact that the subdiffusive behavior is only seen when the band edge does not lie inside any other energy band of the wire, suggests that a transition in the behaviour of the conductance from ballistic to subdiffusive behavior can arise as the position of the other bands is changed with respect to the band edge where the Fermi level is set. However, for the Fermi level fixed at some band edge, this edge should remain unaffected as the positions of the other bands are tuned by varying the parameters of H_0 and H_1 . We present a toy example in $2 \times N_x$ ladders in the appendix C where this occurs. In the next section, we discuss that this transition also occurs if $A(\omega)$ has non-trivial topology which is more interesting as we would then expect the subdiffusive behaviour to be protected from the effects of weak disorder in $A(\omega)$.

V. TOPOLOGICALLY NON-TRIVIAL $A(\omega)$

Let us order $\lambda_k(\omega)$ such that $\lambda_1 < \lambda_2 < \lambda_3 < \dots < \lambda_{N_y}$. As per the subdiffusive condition, we must have for some $k = k^*$, $|\lambda_{k^*}| = 2$ and simultaneously $|\lambda_{k \neq k^*}| > 2$. If $\lambda_{k^*} = 2$, then latter part of the condition is not a problem for $k > k^*$, those eigenvalues are by definition bigger than λ_{k^*} . In order to have $|\lambda_{k < k^*}| > 2$, λ_{k^*} should be gapped from below with a gap strength of at least 4. Similar arguments for $\lambda_{k^*} = -2$ would give that it should be gapped from above. We fix $\lambda_{k^*} = 2$ to avoid any confusions. This required structure in the spectrum of the matrix $A(\omega)$ has a striking similarity with 1D insulators of nontrivial topology where the gap could be tuned keeping the topological modes at a fixed eigenvalue. Let us now fix $\omega = 0$ for simplicity, so we choose $A(\omega = 0)$ to have a non-trivial topology and fix $\lambda_{k^*}(\omega = 0) = 2$ to correspond to a topological mode. Then a transition from ballistic to subdiffusive behavior in the conductance at $\omega = 0$ should take place as the gap between the topological mode and the other eigenvalues lower than it becomes greater than 4. This transition is possible as the topological modes stay at fixed energy as the gap is tuned by changing the parameters of $A(\omega = 0)$. In terms of the energy bands of the wire this transition is understood as follows: Since $A(\omega = 0)$ has fixed eigenvalues of magnitude 2, $\omega = 0$ corresponds to a band edge of the energy

bands of the isolated wire. The tuning of the gap between the λ_{k^*} and the eigenvalues smaller than λ_{k^*} , corresponds to shifting the position of the other energy bands of the wire with respect to the band edge at $\omega = 0$. Then, if $\omega = 0$ does not lie within any other energy band of the wire, the behavior of the conductance is subdiffusive. If $\omega = 0$ lies with the other energy bands of the wire, then their ballistic contribution dominates the behavior of the conductance.

We refer to the subdiffusive behavior arising from topological modes as topological subdiffusive behavior to separate it from the subdiffusive behavior, that happens at the band edges of the wire due to non topological modes of $A(\omega)$, even though the underlying cause for the two is the same. The reason for such a distinction is that the topological subdiffusive behavior due to the topological modes is protected from weak disorders in $A(\omega)$. However, a fine tuning of the Fermi level around $\omega = 0$ is required to see the subdiffusive behavior as the disorder may change the energy of the topological modes by some small amounts. Basically, the subdiffusive behavior enjoys the same topological protection as the modes themselves. In contrast, the trivial subdiffusive behavior arises due to the trivial modes at the band edges of the wire. In the topologically trivial parameter regimes of $A(\omega = 0)$, since the topological modes are absent, a usual transition from ballistic to exponential decay in the behavior of the conductance takes place as the gap strength is tuned across the value 4. This is less interesting as this transition occurs because $\omega = 0$ lies within the energy bands of the isolated wire and out of the energy bands of the isolated wire for the ballistic and exponential decaying conductance, respectively.

The transition points of the two transitions are equally interesting even if the exponential transition is of less interest than the subdiffusive transition. The reason is that at these points the bands of the bulk spectrum of $A(\omega = 0)$ touch the value 2 and therefore become trivially subdiffusive eigenvalues. Their contribution to the conductance should therefore be taken into account as their interplay with the topological subdiffusive eigenvalues/exponential eigenvalues could lead to different behaviors of the conductance. This is illustrated in the next section where we numerically compute conductance of a simple model and find that as $N_y \rightarrow \infty$, the conductance shows a $1/N_x^3$ subdiffusive behavior. We also verify the existence of the topological subdiffusive behavior for this model.

VI. BALLISTIC TO SUBDIFFUSIVE TRANSITION FOR A TWO-DIMENSIONAL MODEL OF SSH-CHAINS

We choose $H_1 = \eta I$, and $H_0 = 2\eta I + H_{SSH}$, where H_{SSH} is the Hamiltonian of the SSH chain given by,

$$H_{SSH}[y, y'] = t_1 \delta_{y, y'-1} + t_2 \delta_{y, y'+1}, \quad (30)$$

where $t_1, t_2 > 0$ are the hopping parameters of the chain. So, we are basically connecting SSH chains to each other via a simple hopping matrix to form the 2D wire. The spectrum of the isolated wire at finite N_y , but $N_x \rightarrow \infty$ is given by diagonalizing the matrix $2\eta I + H_{SSH} + 2\eta \cos(k_x)$ at each value of the wave vector $k_x \in (-\pi, \pi)$. Since, for large N_y , H_{SSH} has two eigenvectors of zero energy in the topological regime ($t_2 > t_1$), which are gapped from the bulk spectrum with the gap $|t_2 - t_1|$. Correspondingly, $A(\omega = 0)$ also has fixed eigenvalues at 2, with the same gap strength. We, therefore, expect the subdiffusive transition in the conductance at $\omega = 0$ for large N_y with the transition point given by $t_2 = t_1 + 4\eta$. For all $t_2 > 4\eta + t_1$, the conductance is expected to scale subdiffusively as $1/N_x^2$ while for $t_2 < 4\eta + t_1$ some of the eigenvalues of $A(\omega = 0)$ will have magnitude less than 2, and correspondingly the conductance will show a ballistic behavior with N_x . Note that the subdiffusive phase is deep within the topological phase of the SSH chain ($t_2 > t_1$), and since the topological modes are necessary to see subdiffusive behavior, such a transition is absent in the parameter regimes corresponding to the topologically trivial phase of the SSH chain ($t_1 > t_2$), we expect an exponential transition in the behavior of the conductance with the transition point $t_1 = t_2 + 4\eta$.

Note that $\omega = 0$ lies at the edge of the band given by $2\eta + 2\eta \cos(k_x)$ of the isolated wire. This is due to the fact that H_1 is trivial, and therefore commutes with H_0 . So, we are looking at the conductance with the Fermi level at the band edges of the isolated wire. The transitions could also be understood as whether or not $\omega = 0$ lies within other energy bands of the isolated wire. If $\omega = 0$ does not lie within the other energy bands of the isolated wire, the dominant contribution is the subdiffusive contribution from the band edge at $\omega = 0$. However, if $\omega = 0$ lies within the other bands of the isolated wire, the ballistic contribution due to the other bands dominates the behaviour of the conductance. In the topologically trivial regime of the SSH chain, the topological modes are absent so the subdiffusive behavior is replaced by an exponential behavior.

A. Numerical results

For numerical computations we set $\eta = 1$ and take the intra-chain reservoir Hamiltonian, \tilde{H}_0 to just allow nearest neighbor hoppings with hopping strength, η_{by} . Using this choice of \tilde{H}_0 , a numerical computation of the conductance at $\omega = 0$ in the topological and trivial parameter regimes of the SSH chain is shown in Fig. 2 and Fig. 3, respectively. We also show the corresponding plots of the absolute value of the spectrum of $A(\omega)$ in Fig. (2) which we do not show for Fig. (3) as they look same as in Fig. (2) except that the eigenvalues corresponding to the topological modes, lying on the dotted line, are absent. From Fig. (2a), we see that the conductance

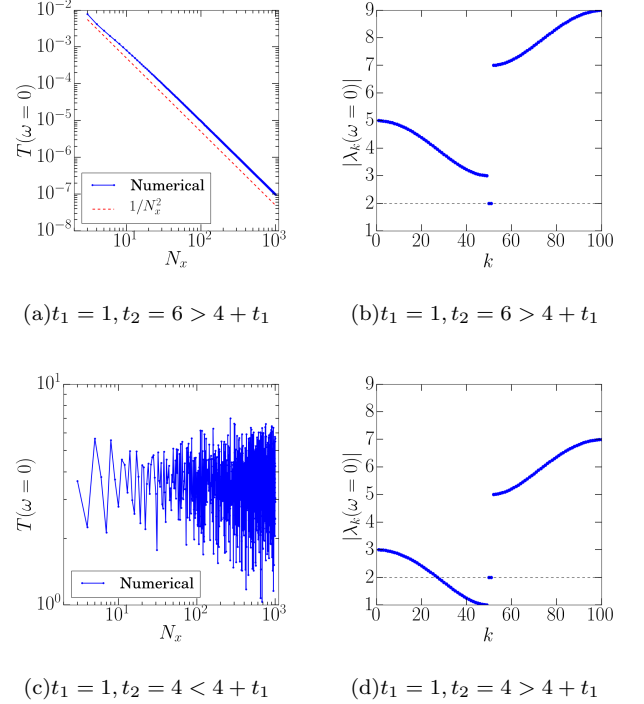


FIG. 2. Conductance plots, *log-log scale*, in the topological regime of the SSH chain with $\eta = 1$, $\eta_c = 0.5$, $\eta_{bx} = \eta_{by} = 2$, and $N_y = 100$. (a) and (c) corresponds to the subdiffusive parameter regime, and the ballistic parameter regime, respectively. (b) and (d) are the corresponding plots of the absolute value of the spectrum of the matrix $A(\omega = 0)$. We see that the numerical results show the transition from ballistic to subdiffusive as expected from the theory.

goes down as $1/N_x^2$ for $t_2 > 4\eta + t_1$ as expected from the theory. The corresponding plots for the spectrum in Fig. (2b) has all eigenvalues of magnitude greater than 2 except for the topological modes which lie on the dotted line at the value 2. In Fig. (2c), a ballistic behavior of the conductance is observed as $t_2 < 4\eta + t_1$. The ballistic contribution comes from the eigenvalues in Fig. (2d) which are below the dotted line. Similarly, in Fig. (2a) and Fig. (2b) we see an exponentially decaying and ballistic behaviour of the conductance for $t_1 > 4\eta + t_2$ and $t_1 < 4\eta + t_2$, respectively. The subdiffusive behavior is replaced by the ballistic behavior as the topological modes are absent in this parameter regime.

If a small disorder is added to the SSH chain, we expect the subdiffusive behavior to persist. However, the small amounts of change in the energy of the topological modes should be compensated by a small shift in the Fermi level. To understand this, let us assume that the disorder shifts the energy of the topological modes of $A(\omega = 0)$ by a small amount δ , and let $k = k^*$ correspond to this eigenvalue of $A(\omega = 0)$. We then have,

$$p_{N_x}^{k^*} = \frac{1}{\sin(q^{k^*})} \sin(q^{k^*}(N_x + 1)), \quad (31)$$

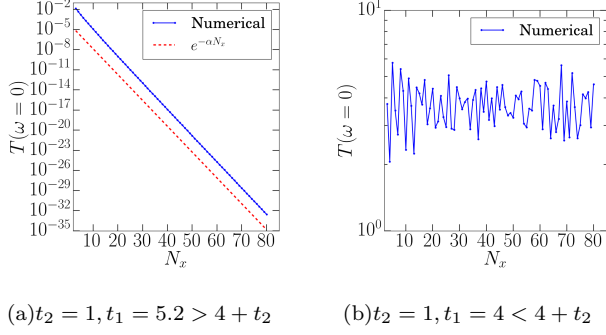


FIG. 3. Conductance plots, *log-linear scale*, in the trivial regime of the SSH chain with $\eta = 1$, $\eta_c = 0.5$, $\eta_{bx} = \eta_{by} = 2$, and $N_y = 100$. (a) and (b) correspond to the parameter regimes of exponential decay, and the ballistic behavior of the conductance, respectively. The numerical results show the transition from ballistic to exponential decay.

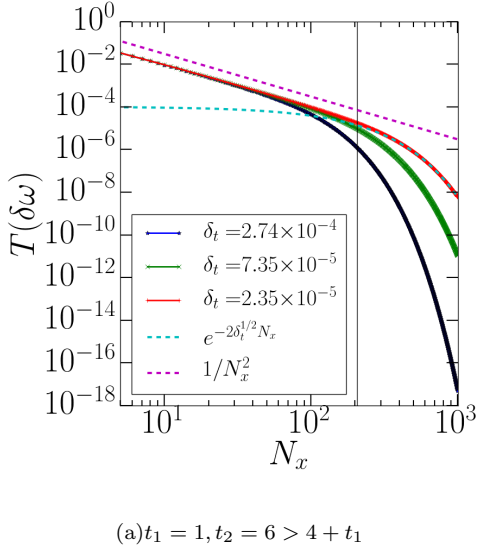


FIG. 4. Conductance at different Fermi levels $\delta\omega = \delta - \delta_t$ in presence of the onsite disorder in the chemical potential of the SSH chain. The chemical potential at each site is chosen randomly from the interval $(2 - \delta\mu, 2 + \delta\mu)$, $\delta\mu = 0.1$. We see that as the Fermi level is finely tuned, $1/N_x^2$ behavior is observed till system sizes of order $N_x \sim 1/\delta_t^{1/2}$. This is seen from the red curve where the vertical line is drawn at $N_x = 1/\delta_t^{1/2}$. The conductance shows a behavior of $1/N_x^2$ for $N_x \ll 1/\delta_t^{1/2}$ and $e^{-2\delta_t^{1/2}N_x}$ for $N_x \gg 1/\delta_t^{1/2}$. Parameter values— $\eta = 1$, $\eta_c = 0.5$, $\eta_{bx} = \eta_{by} = 2$, and $N_y = 200$.

where, $q^{k*} = \arccos \frac{2+\delta}{2}$. In order to understand the behaviour at finite N_x , we consider the expansion of p_N^{k*} in terms of δ . We have,

$$q^{k*} = \arccos \frac{2+\delta}{2} = i(\delta^{1/2} - \frac{1}{4!}\delta^{3/2} + \dots), \quad (32)$$

and, therefore,

$$p_{N_x}^{k*} = \frac{\sinh[\tilde{\delta} - \frac{1}{4!}\frac{\tilde{\delta}^3}{N_x^2} + \dots]}{\sinh[\frac{\tilde{\delta}}{N_x} - \frac{1}{4!}\frac{\tilde{\delta}^3}{N_x^3} + \dots]}, \quad (33)$$

where $\tilde{\delta} = \delta^{1/2}N_x$, and we replaced $N_x + 1$ by N_x . We see that if $\tilde{\delta} \ll 1$, then the leading contribution in Eq. (33) is given by $p_{N_x}^{k*} \sim N_x$. The latter implies that the conductance $T(\omega = 0) \sim 1/N_x^2$. We therefore see that at a finite N_x , the conductance shows a behaviour of $1/N_x^2$ provided $\delta \ll 1/N_x^2$. On the other hand, if $\tilde{\delta} \gg 1$, then the leading contribution in Eq. (33) is given by $p_{N_x}^{k*} \sim e^{\delta^{1/2}N_x}$. This leads to exponentially decaying or ballistic behavior of the conductance as $e^{-2\delta^{1/2}N_x}$ for $\delta > 0$ or $\delta < 0$, respectively. Now, if the Fermi level ω is shifted to $\delta\omega$ from $\omega = 0$, then the total shift in the eigenvalue corresponding to the topological mode of $A(\omega)$ is given by, $\delta_t = \delta - \delta\omega$. We show in Fig. (4) the behavior of the conductance computed numerically at different values of δ_t . The vertical line in the plot is drawn at $N_x = 1/\delta_t^{1/2}$, where δ_t corresponds to the red curve of the plot. The numerical calculations agree with $1/N_x^2$ and $e^{-2\delta_t^{1/2}N_x}$ for $\delta_t \ll 1/N_x^2$ and $\delta_t \gg 1/N_x^2$, respectively.

We now present the results at the transition points of the two transitions. The asymptotic behaviors of conductance with the wire size are shown in Fig. 5. We observe a crossover from $1/N_x^3$ to $1/N_x^2$ at the subdiffusive transition point and to $e^{-\alpha N_x}/N_x^3$ at exponential transition point, respectively. The crossover region shifts towards larger values of N_x as N_y is increased. Therefore in the limit of $N_y \rightarrow \infty$, the numerical results indicate a subdiffusive scaling of $1/N_x^3$ for both the transition points. A careful study of the conductance at the transition points is required to explain these behaviors. We expect that these interesting behaviors arise due the interplay of the contribution of the three types of eigenvalues of $A(\omega = 0)$, namely topologically subdiffusive, trivially subdiffusive and exponential eigenvalues. This happens because the edges of the bulk bands of $A(\omega)$ also contribute subdiffusively as they lie at the value 2. We see this in Fig. (5b) and Fig. (5c) for the subdiffusive and exponential transition point, respectively.

VII. CONCLUSION

In conclusion, we investigated the possibility of universal subdiffusive transport in a 2D fermionic wire defined on a square lattice. We find that such a behavior occurs at the values of the Fermi level, ω , where the matrix $A(\omega) = (-\omega + H_0)H_1^{-1}$ has at least one eigenvalue of magnitude 2 while all other eigenvalues are of magnitude greater than 2. We have shown that this implies that ω lies at the edge of an energy band of the isolated wire that does not lie within any other energy band.

We pointed out that the condition for observing the subdiffusive behavior can be simply satisfied by choosing

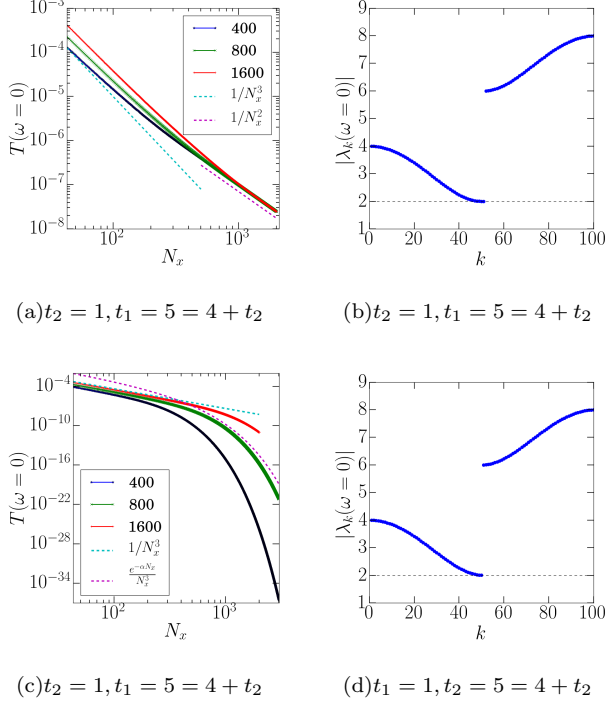


FIG. 5. Conductance, *log-log scale*, and spectrum of $A(\omega = 0)$ at the transition points of the subdiffusive(a,b) and exponential(c,d) transitions of the SSH chain. We see a scaling of $1/N_x^3$ as $N_y \rightarrow \infty$ for both transition points, and at finite N_y we observe a crossover from $1/N_x^3$ to $1/N_x^2$ and to $e^{-\alpha N_x}/N_x^3$ at the subdiffusive and exponential transition points, respectively. Other parameter values are $\eta_c = 0.5$ and $\eta_{bx} = \eta_{by} = 2$.

$A(\omega)$ such that it has a non-trivial bulk topology. For such a case, the conductance shows a ballistic to subdiffusive transition asymptotically with respect to N_x , provided that the eigenvalues corresponding to the topological modes are fixed at an absolute value of 2. The latter corresponds to the Fermi level ω at a band edge of the isolated wire. Therefore, the transition occurs as the positions of the other bands of the isolated wire are tuned with respect to the band edge where the Fermi level is set. Since the subdiffusive behavior arises due to the topological modes, it enjoys the same topological protection as the modes themselves. The transition point of the ballistic to subdiffusive behavior lies inside the parameter regimes where $A(\omega)$ has a nontrivial topology. In parameter regimes corresponding to the topologically trivial phase of $A(\omega)$, the conductance shows a usual transition from ballistic to exponentially decaying behavior with respect to N_x .

Interestingly, at the transition points corresponding to

subdiffusive and exponential transitions different behaviors of the conductance with respect to N_x may arise for finite and thermodynamically large N_y . This is because at these points the edges of the bulk bands of $A(\omega)$ become subdiffusive and their interplay with the topologically subdiffusive modes/exponential modes may lead to different N_x dependence of the conductance at finite and thermodynamically large N_y .

We illustrate the theoretical predictions in a simple model by choosing $H_1 = \eta I$ and H_0 to correspond to the hopping matrix of the SSH chain with a constant chemical potential. The chemical potential is added so that the eigenvalues corresponding to the topological modes of $A(\omega)$ lie at the value 2. For this model, the transition points of the subdiffusive and exponential transitions are given by $t_1 = t_2 + 4\eta$ and $t_2 = t_1 + 4\eta$, respectively. t_1 , and t_2 are the hopping parameters of the SSH chain. We then compute the conductance of this model numerically and the results indicate the following for the conductance at $\omega = 0$ for this simple model:

- A transition from ballistic to subdiffusive behaviour ($1/N_x^2$) at any finite but large N_y inside the topological regime.
- A transition from ballistic to exponentially decaying behavior at any finite N_y inside the topologically trivial regime.
- For finite N_y , the conductance shows a crossover from $1/N_x^3$ to $1/N_x^2$ at the subdiffusive transition point and to $e^{-\alpha N_x}/N_x^3$ at the exponential transition point, respectively. However, as N_y is increased the crossover region happens for larger values of N_x . Therefore, the subdiffusive behavior ($1/N_x^3$) persists in the limit $N_y \rightarrow \infty$.

The results from the numerical computations of the conductance agree well with the theory away from the transition points, but a careful study of the conductance at the transition points is required to explain its behavior at these points.

In this paper, we only looked at a specific example of a Hermitian $A(\omega)$ having nontrivial topology. However, it may be possible to engineer models with non-Hermitian $A(\omega)$, as pseudo Hermitian matrices have been known to have non-trivial topology^{41–45}.

VIII. ACKNOWLEDGEMENTS

I thank Marko Žnidarič, Kevin Kavanagh, and Jaš Bensa for useful discussions. The computations for the largest system size were done on the TETRIS cluster of ICTS. I also acknowledge support by Grant No. J1-4385 from the Slovenian Research Agency.

- ¹ Supriyo Datta, *Electronic transport in mesoscopic systems* (Cambridge university press, 1997).
- ² Y Imry, "Introduction to mesoscopic physics oxford up," New York (1997).
- ³ M. Büttiker, Y. Imry, R. Landauer, and S. Pinhas, "Generalized many-channel conductance formula with application to small rings," *Phys. Rev. B* **31**, 6207–6215 (1985).
- ⁴ Abhishek Dhar and Diptiman Sen, "Nonequilibrium green's function formalism and the problem of bound states," *Physical Review B* **73**, 085119 (2006).
- ⁵ Adhip Agarwala and Vijay B. Shenoy, "Topological insulators in amorphous systems," *Phys. Rev. Lett.* **118**, 236402 (2017).
- ⁶ Zheng-Rong Liu, Chun-Bo Hua, Tan Peng, and Bin Zhou, "Chern insulator in a hyperbolic lattice," *Phys. Rev. B* **105**, 245301 (2022).
- ⁷ Tan Peng, Chun-Bo Hua, Rui Chen, Dong-Hui Xu, and Bin Zhou, "Topological anderson insulators in an ammann-beenker quasicrystal and a snub-square crystal," *Phys. Rev. B* **103**, 085307 (2021).
- ⁸ Dibyendu Roy, CJ Bolech, and Nayana Shah, "Majorana fermions in a topological superconducting wire out of equilibrium: Exact microscopic transport analysis of a p-wave open chain coupled to normal leads," *Physical Review B* **86**, 094503 (2012).
- ⁹ Nilanjan Bondyopadhyaya and Dibyendu Roy, "Nonequilibrium electrical, thermal and spin transport in open quantum systems of topological superconductors, semiconductors and metals," (2020), arXiv:2010.08336 [cond-mat.mes-hall].
- ¹⁰ Junaid Majeed Bhat and Abhishek Dhar, "Transport in spinless superconducting wires," *Phys. Rev. B* **102**, 224512 (2020).
- ¹¹ R Shankar, "Topological insulators—a review," arXiv preprint arXiv:1804.06471 (2018).
- ¹² M Zahid Hasan and Charles L Kane, "Colloquium: topological insulators," *Rev. Mod. Phys.* **82**, 3045 (2010).
- ¹³ Joel E Moore, "The birth of topological insulators," *Nature* **464**, 194–198 (2010).
- ¹⁴ C. L. Kane and E. J. Mele, " Z_2 topological order and the quantum spin hall effect," *Phys. Rev. Lett.* **95**, 146802 (2005).
- ¹⁵ Liang Fu, C. L. Kane, and E. J. Mele, "Topological insulators in three dimensions," *Phys. Rev. Lett.* **98**, 106803 (2007).
- ¹⁶ Wu-Pei Su, John Robert Schrieffer, and Alan J Heeger, "Solitons in polyacetylene," *Physical review letters* **42**, 1698 (1979).
- ¹⁷ Daichi Obana, Feng Liu, and Katsunori Wakabayashi, "Topological edge states in the su-schrieffer-heeger model," *Phys. Rev. B* **100**, 075437 (2019).
- ¹⁸ A Yu Kitaev, "Unpaired majorana fermions in quantum wires," *Physics-Uspekhi* **44**, 131 (2001).
- ¹⁹ F. D. M. Haldane, "Model for a quantum hall effect without landau levels: Condensed-matter realization of the "parity anomaly"," *Physical review letters* **61**, 2015–2018 (1988).
- ²⁰ B Andrei Bernevig, Taylor L Hughes, and Shou-Cheng Zhang, "Quantum spin hall effect and topological phase transition in hgte quantum wells," *Science* **314**, 1757–1761 (2006).
- ²¹ Gregor Jotzu, Michael Messer, Rémi Desbuquois, Martin Lebrat, Thomas Uehlinger, Daniel Greif, and Tilman Esslinger, "Experimental realization of the topological haldane model with ultracold fermions," *Nature* **515**, 237–240 (2014).
- ²² Markus König, Steffen Wiedmann, Christoph Brüne, Andreas Roth, Hartmut Buhmann, Laurens W Molenkamp, Xiao-Liang Qi, and Shou-Cheng Zhang, "Quantum spin hall insulator state in hgte quantum wells," *Science* **318**, 766–770 (2007).
- ²³ Madhumita Saha, Bijay Kumar Agarwalla, Manas Kulkarni, and Archak Purkayastha, "Universal subdiffusive behavior at band edges from transfer matrix exceptional points," *Phys. Rev. Lett.* **130**, 187101 (2023).
- ²⁴ Madhumita Saha, Manas Kulkarni, and Bijay Kumar Agarwalla, "Exceptional hypersurfaces of transfer matrices of finite-range lattice models and their consequences on quantum transport properties," *Phys. Rev. B* **108**, 075406 (2023).
- ²⁵ Y Last, "A relation between ac spectrum of ergodic jacobi matrices and the spectra of periodic approximants," *Communications in mathematical physics* **151**, 183–192 (1993).
- ²⁶ Luca Molinari, "Transfer matrices and tridiagonal-block hamiltonians with periodic and scattering boundary conditions," *Journal of Physics A: Mathematical and General* **30**, 983 (1997).
- ²⁷ Luca Molinari, "Transfer matrices, non-hermitian hamiltonians and resolvents: some spectral identities," *Journal of Physics A: Mathematical and General* **31**, 8553 (1998).
- ²⁸ David H Dunlap, HL Wu, and Philip W Phillips, "Absence of localization in a random-dimer model," *Physical Review Letters* **65**, 88 (1990).
- ²⁹ Craig Pryor and A Zee, "Electron hopping in the presence of random flux," *Physical Review B* **46**, 3116 (1992).
- ³⁰ Tohru Kawarabayashi and Tomi Ohtsuki, "Diffusion of electrons in random magnetic fields," *Physical Review B* **51**, 10897 (1995).
- ³¹ Eugene P Wigner, "Normal form of antiunitary operators," *Journal of Mathematical Physics* **1**, 409–413 (1960).
- ³² W Pauli, "On dirac's new method of field quantization," *Reviews of Modern Physics* **15**, 175 (1943).
- ³³ John L Cardy, "Conformal invariance and the yang-lee edge singularity in two dimensions," *Physical review letters* **54**, 1354 (1985).
- ³⁴ Patrick Dorey, Clare Dunning, and Roberto Tateo, "Spectral equivalences, bethe ansatz equations, and reality properties in PT-symmetric quantum mechanics," *Journal of Physics A: Mathematical and General* **34**, 5679 (2001).
- ³⁵ Ali Mostafazadeh, "Pseudo-hermiticity versus pt symmetry: the necessary condition for the reality of the spectrum of a non-hermitian hamiltonian," *Journal of Mathematical Physics* **43**, 205–214 (2002).
- ³⁶ Ali Mostafazadeh, "Pseudo-hermiticity versus pt-symmetry. ii. a complete characterization of non-hermitian hamiltonians with a real spectrum," *Journal of Mathematical Physics* **43**, 2814–2816 (2002).
- ³⁷ Michael E Fisher, "Yang-lee edge singularity and ϕ^3 field theory," *Physical Review Letters* **40**, 1610 (1978).
- ³⁸ Yuto Ashida, Zongping Gong, and Masahito Ueda, "Non-hermitian physics," *Advances in Physics* **69**, 249–435 (2020).

- ³⁹ GD Mahan, “Many-particle physics (kluwer, new york, 2000).” .
- ⁴⁰ Georgo Metalidis, “Electronic transport in mesoscopic systems,” Verlag nicht ermittelbar (2007).
- ⁴¹ Tony E Lee, “Anomalous edge state in a non-hermitian lattice,” Physical review letters **116**, 133903 (2016).
- ⁴² Yong Xu, Sheng-Tao Wang, and L-M Duan, “Weyl exceptional rings in a three-dimensional dissipative cold atomic gas,” Physical review letters **118**, 045701 (2017).
- ⁴³ Yi Chen Hu and Taylor L Hughes, “Absence of topological insulator phases in non-hermitian p t-symmetric hamiltonians,” Physical Review B **84**, 153101 (2011).
- ⁴⁴ Henning Schomerus, “Topologically protected midgap states in complex photonic lattices,” Optics letters **38**, 1912–1914 (2013).
- ⁴⁵ Simon Lieu, “Topological phases in the non-hermitian suschrieffer-heeger model,” Physical Review B **97**, 045106 (2018).

Appendix A: General Conditions for Ballistic, Subdiffusive and Exponential Behaviour

Let $\lambda_k = a_k + ib_k$, where a_k and b_k are real, be the eigenvalues of the matrix $A(\omega)$. Then,

$$q^k = \arccos\left(\frac{a_k + ib_k}{2}\right) \quad (\text{A1})$$

$$= \cosh^{-1} \xi_-(a_k, b_k) + i \cosh^{-1} \xi_+(a_k, b_k), \quad (\text{A2})$$

where,

$$\xi_{\pm}(a_k, b_k) = \frac{1}{2} \left[\sqrt{\left(\frac{a_k}{2} + 1\right)^2 + \frac{b_k^2}{4}} \pm \sqrt{\left(\frac{a_k}{2} - 1\right)^2 + \frac{b_k^2}{4}} \right]. \quad (\text{A3})$$

Let us now discuss the three cases for the behaviour of the conductance separately,

- **Ballistic:** For the conductance to behave ballistically, we must have atleast one eigenvalue λ_k for which the imaginary part of q^k vanishes. Therefore, at least one of the eigenvalues should have real and imaginary parts which lie on the curve, $\xi_+(a, b) = 1$, in the ab plane. This equation simply implies that $b = 0$ and $-2 < a < 2$. So, the condition for the ballistic behavior remains the same as in the case of real spectrum of $A(\omega)$.
- **Exponential:** For the exponential behavior, the imaginary part of all q^k must survive. So, no eigenvalue of $A(\omega)$ should lie on the real line between -2 and 2 . Hence, the contribution due to the imaginary eigenvalues is always exponentially small in N_x .
- **Subdiffusive:** This behavior comes from the non-diagonalizability of the matrix, $M = \begin{pmatrix} \lambda_k & 1 \\ -1 & 0 \end{pmatrix}$. This only happens for $\lambda_k = 2$. Then the condition for the sub diffusive behavior is that no eigenvalue

should lie on the real line between -2 and 2 and simultaneously at least one of the eigenvalues should be of magnitude 2 .

It is straight forward to see if $\lambda_k(\omega)$'s are real the conditions discussed in the main text for real spectrum of $A(\omega)$ are reproduced. Note that the conditions for observing the three behaviors of the conductance are not very different from the case of real spectrum of $A(\omega)$, therefore all the complex values of $A(\omega)$ are irrelevant.

Appendix B: Eigenvalues of absolute value 2 only at the band edges of the isolated wire

To show that the edges of the energy bands of the isolated wire always contribute subdiffusively, we need to show that $A(\omega)$ has eigenvalues of absolute value 2 at ω equal to the band edges. We first find a correspondence between eigenvalues of the matrix $A(\omega)$ and the energy eigenvalues of the isolated wire. The latter is given by diagonalizing the matrix, $H_0 + 2H_1 \cos k_x$, $k_x \in (-\pi, \pi)$. The characteristic polynomial of this matrix is given by,

$$\det[H_0 + 2H_1 \cos k_x - \epsilon] = \det[(A(\omega) + 2 \cos k_x)H_1 + \omega - \epsilon], \quad (\text{B1})$$

where $\det[\cdot]$ denotes the determinant of the matrix. Clearly, for the Fermi level, ω , exactly equal to one of the energy eigenvalues of the isolated wire, $\epsilon(k_x)$, the above determinant reads, $\det[A(\omega = \epsilon(k_x)) + 2 \cos k_x] \det[H_1]$, which vanishes for $\lambda_k = -2 \cos k_x$. Therefore, a particular energy eigenvalue of the isolated system, $\epsilon(k_x)$, would correspond to that eigenvalue λ_k of $A(\omega = \epsilon(k_x))$ for which $\lambda_k = -2 \cos(k_x)$. We see that the eigenvalues of $A(\omega)$ which correspond to the energies within the bands of the system have an absolute value less than 2 for arbitrary H_0 and H_1 . Using this correspondence, we also see that $\lambda_k = \pm 2$, corresponds to $k_x = -\pi, 0, \pi$. These values of k_x correspond to the band edges of the isolated wire. As, at these points,

$$\frac{\partial \epsilon(k_x)}{\partial k_x} \sim \langle \psi_{\epsilon(k_x)} | H_1 | \psi_{\epsilon(k_x)} \rangle \sin(k_x), \quad (\text{B2})$$

where $|\psi_{\epsilon(k_y)}\rangle$ is the eigenstate corresponding to $\epsilon(k_y)$, vanishes.

Appendix C: A toy example with $[H_0, H_1] \neq 0$

To construct an example, let us work in the diagonal basis of H_1 , with $N_y = 2$. We are free to choose eigenvalues of H_1 , we take them to be μ_1 and μ_2 . We also fix $\omega = 0$ for simplicity, and denote $A(\omega = 0)$ as A . Therefore a general A which is H_1 -pseudo Hermitian is given by,

$$A = \begin{pmatrix} A_{11} & A_{12} \\ \frac{\mu_2}{\mu_1} A_{12}^* & A_{22} \end{pmatrix}, \quad (\text{C1})$$

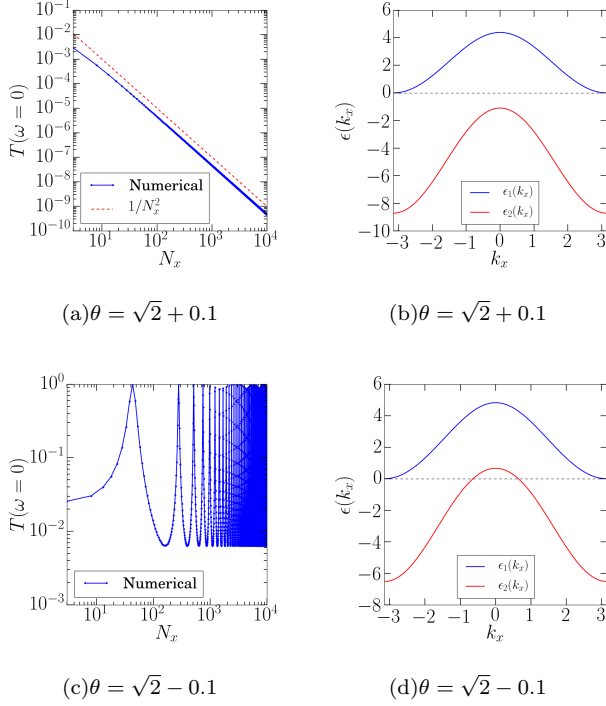


FIG. 6. Conductance, *log-log scale*, at zero Fermi level for the toy model at $\theta = \sqrt{2} \pm 0.1$ and the corresponding plots for the spectrum of the wire. A transition from ballistic to subdiffusive behavior is seen as θ is tuned across the region where its absolute value is $\sqrt{2}$. Other parameter values are $\eta_c = 0.5$ and $\eta_{bx} = \eta_{by} = 2$.

where A_{11} and A_{22} are real. Consequently, H_0 is given by,

$$H_0 = \begin{pmatrix} A_{11}\mu_1 & A_{12}\mu_2 \\ A_{12}^*\mu_2 & A_{22}\mu_2 \end{pmatrix}. \quad (C2)$$

Let us now use the free parameters of A to get an eigenvalue of 2. A simple case would be to consider $\mu_1 = 1$

and $\mu_2 = 2$ and A to be of the form,

$$A = \begin{pmatrix} \theta & 1 \\ 2 & 2\frac{\theta-1}{\theta-2} \end{pmatrix}, \quad \theta \neq 2. \quad (C3)$$

The eigenvalues of this choice of A are 2 and $\frac{2}{\theta-2} + \theta$. With this A and H_1 , H_0 is given by,

$$H_0 = \begin{pmatrix} \theta & 2 \\ 2 & 4\frac{\theta-1}{\theta-2} \end{pmatrix}. \quad (C4)$$

We note that A will always have an eigenvalue of absolute value 2, albeit the other eigenvalue is of magnitude less than 2 only if $|\theta| < \sqrt{2}$. This means a ballistic to subdiffusive transition in the behavior of the conductance at zero Fermi level would occur as θ is tuned outside the region where $|\theta| < \sqrt{2}$. A numerical computation of the conductance verifies this transition, and can be seen from Fig. (6a) and Fig. (6c). Fig. (6a) is for $|\theta| > 2$ and Fig. (6c) is for $|\theta| < 2$, and the two figures show a subdiffusive and ballistic behavior of the conductance, respectively.

This transition could be understood more physically in terms of the energy eigenstates of the system. Since $N_y = 2$, the wire has two energy bands given by, $\epsilon_1(k_x)$ and $\epsilon_2(k_x)$. These are given by the eigenvalues of the matrix, $H_0 + 2H_1 \cos(k_x)$. Now as at $\omega = 0$, $A(\omega)$ has an eigenvalue of magnitude 2 for all values of $\theta \neq 2$, the edge of one of the energy bands, say $\epsilon_1(k_x)$, is fixed at $\omega = 0$. If $|\theta| < \sqrt{2}$ then $\omega = 0$ lies inside the other band, $\epsilon_2(k_x)$, and therefore its ballistic contribution dominates the transport. Outside this range of values for θ , $\omega = 0$ lies outside the other band, and therefore the only contribution is the subdiffusive contribution of the band edge of $\epsilon_1(k_x)$. These features can be seen from the spectrum of the wire for $|\theta| > 2$ and $|\theta| < 2$ in Fig. (6b) and Fig. (6c), respectively.